Supporting information

Alexander E. J. Hoffman, Jelle Wieme, Sven M. J. Rogge, Louis Vanduyfhuys, and Veronique Van Speybroeck*

The impact of lattice vibrations on the macroscopic breathing behavior of MIL-53(Al)

S1 Derivation of volume-frequency relations

The volume-frequency relations cannot be constructed by simply ordering the vibrational frequencies according to their magnitude at each volume and assuming that this order remains constant as this will neglect possible mode crossings. To overcome this issue, a measure of similarity between two modes of structures at different unit cell volume has to be employed. A possible measure of similarity between two vibrational modes is the scalar product of their eigenvectors (see also Ref. [1]):

$$c_{ij}^{\alpha\beta} = \boldsymbol{v}_i^{\alpha} \cdot \boldsymbol{v}_j^{\beta} \tag{S1}$$

Here, $\boldsymbol{v}_i^{\alpha}$ represents the eigenvector of mode i at volume α. As all normal modes at a given unit cell volume are orthonormal with respect to each other, the following relation holds:

$$c_{ii}^{\alpha\beta} = \boldsymbol{v}_i^{\alpha} \cdot \boldsymbol{v}_i^{\beta} = \delta_{\alpha\beta} \tag{S2}$$

Consequently, the scalar product of the eigenmodes of structures at neighboring unit cell volumes will yield values close to one when these eigenmodes have a high degree of similarity. Otherwise, this scalar product will be negligibly small.

Using the scalar product as a similarity measure, there are still multiple ways of connecting the vibrational modes over the computed volume range. For example, one could choose a single reference structure and link the eigenmodes of structures

Alexander E. J. Hoffman, Jelle Wieme, Sven M. J. Rogge, Louis Vanduyfhuys, Veronique Van Speybroeck, Center for Molecular Modeling, Ghent University, Technologiepark 46, 9052 Zwijnaarde, Belgium

with different unit cell volumes to the eigenmodes of this particular structure by matching the eigenmodes yielding the highest scalar products. However, this procedure may yield inconsistencies because corresponding eigenmodes can give low values of the scalar product when structures with a large difference in unit cell volume are compared. For instance, this method fails when comparing the equilibrium structures of the CP and LP phase of MIL-53(Al) directly. This can be remedied by comparing the eigenmodes of a structure at a certain unit cell volume with those at the next volume point, as is done in this work. In this way, the deviations between eigenmodes of the same type remain minimal in most cases and they can be matched correctly. Note that, even when using the more elaborate analysis, mode mixing may arise at unit cell volumes where vibrational frequencies cross, which complicates a successful matching.

S2 Effect of dispersion on bond lengths

In the main article, it is mentioned that dispersion forces are, in general, responsible for the increase in vibrational frequencies between the CP and LP phase structures. We investigated the influence of dispersion corrections on the bond strengths by optimizing the geometry of structures at three different volume points (898 $Å^3$, 1150 $Å^3$, and 1399 $Å^3$) without dispersion forces. Afterwards, the corresponding Hessians were calculated following the procedure explained in the computational details. To illustrate the effect of dispersion corrections on the vibrational frequencies and the covalent bond strength, the volume-frequency relations of the aluminum-oxide stretch vibrations are plotted in Figure S1 along with the bond lengths of the aluminum-oxide bonds obtained with and without dispersion corrections. It is clear that at small unit cell volumes dispersion forces have little effect on the bond length and the vibrational frequency. However, at larger unit cell volumes, the bond lengths obtained with dispersion corrections are, in general, smaller compared to those at smaller unit cell volumes. In contrast, without dispersion corrections the bond lengths remain almost unchanged over the considered volume range. Subsequently, the decrease in bond length for increasing unit cell volumes results in an increased vibrational frequency. A possible reason for the small effect of dispersion forces on the bond length at small volumes, despite the fact that they are more prominent in these dense structures, can be found in the high repulsive force which is present when the bonds are shortened in this compressed state.

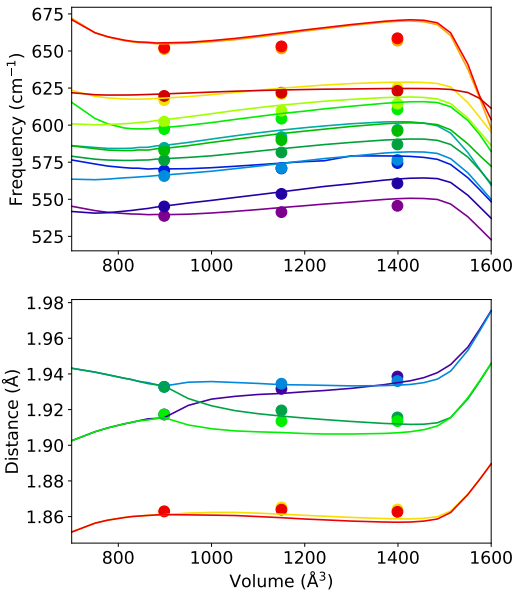

Fig. S1: Top: volume-frequency relations of the vibrational modes describing a stretch of the aluminum-oxide bond. Bottom: length of the aluminum-oxide bonds as a function of the volume. The solid lines represent the results obtained with dispersion corrections, while the dots show the results obtained without dispersion corrections.

S3 IR intensities of modes within the range 300 cm^{-1} – 500 cm^{-1}

Within the range 300 cm^{-1} – 500 cm^{-1}, we observed major changes in the IR spectra as a function of the volume. This could suggest that the normal modes in this range do not follow the general volume-frequency trend. However, in a previous work we dedicated some of the changes in the IR spectra of the CP and the LP phases to alterations within bending modes of the aluminum-oxide backbone [2]. In the LP phase, these modes are coupled with a hydroxyl group rocking vibrations, which makes the modes IR active, whereas in the CP phase, this coupling is not present, which results in an IR inactive mode. As we now dispose of the vibrational frequency and the IR intensity of a certain mode as a function of the volume, we can verify this statement. In Figure S2, the volume-frequency and volume-intensity relations are represented. Almost all

volume-frequency relations follow the general trend as discussed in the manuscript (see Figure S2a). In contrast, the behavior of the volume-intensity relations is more diverse (see Figure S2). For example, consider the bending modes of the aluminum-oxide backbone, which are represented by a solid red and green line in Figure S2b. These modes do indeed have a significant IR activity at the LP volume (1426 Å^3), while they are IR inactive at the CP volume (843 Å^3). The modes become IR active starting from a unit cell volume of 900 Å^3. This specific volume point is not a coincidence. In the distance-volume plots of the aluminum-oxide bonds (Figure S1), we observe a breaking of the symmetry at exactly the same unit cell volume. This results in a distortion of the aluminum-oxide clusters allowing the hydroxyl group to rock. Besides the bending modes of the aluminum-oxide backbone, also other modes show a large change in IR activity over the calculated volume range. This confirms that the change in IR spectra as a function of the volume is a result of differences in IR intensities rather than deviations from the general volume-frequency trend.

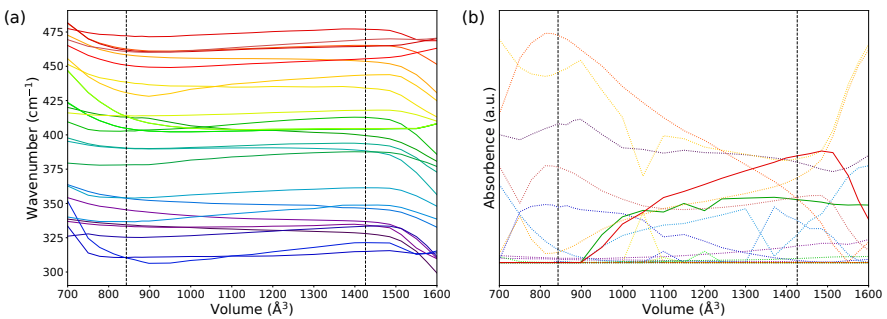

Fig. S2: (a) Volume-frequency relations of the vibrational modes in the range 300-500 cm^{-1}. Dotted lines indicate the equilibrium volumes of the CP and LP phases obtained from electronic structure calculations. (b) IR intensities of the vibrational modes within the range 300 cm^{-1} - 500 cm^{-1} as a function of the volume. The red and green solid line represent the modes where a hydroxyl group starts rocking at a certain unit cell volume, which makes these modes IR active.

S4 Visualization soft modes

In the main manuscript two terahertz vibrations with a monotonically increasing vibrational frequency as a function of the volume are discussed. These modes are referred to as soft modes, as they have very low vibrational frequencies at

low unit cell volumes. The soft mode exhibiting rotations of the aluminum-oxide backbone and translations of the organic linkers is visualized in Figure 4 of the main manuscript. The soft mode exhibiting translations of the aluminum-oxide backbone and rotations of the organic linkers is visualized in Figure S3.

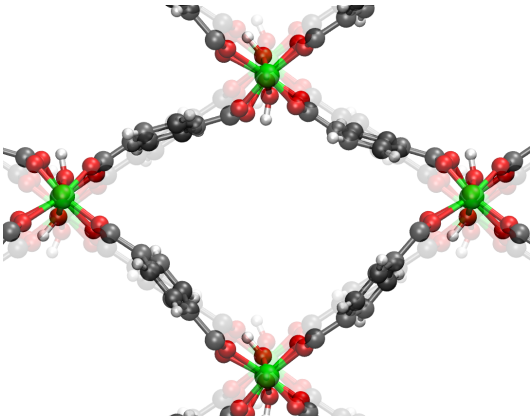

Fig. S3: Visualization of the soft mode exhibiting translations of the aluminum-oxide backbone coupled with rotations of the organic linkers.

S5 Influence of level of theory

In Section 3.2.1 of the main manuscript we discussed the Helmholtz free energy as a function of the volume at different temperatures. These results were obtained by applying the QHA approach at the PBE-D3(BJ) level of theory. From these Helmholtz free energy profiles, the CP phase remained the most stable phase, even for temperatures as high as 500 K, while, experimentally, the LP phase has been shown to be more stable at high temperatures [3]. In this section and according to earlier work [4], it is rationalized that this deviation between theory and experiment is a consequence of an incorrect prediction of the electronic energy rather than an erroneous calculation of the lattice vibrations.

First, the electronic energy can be described at a higher level of theory. For example, it is possible to apply the random-phase approximation (RPA), which results in a more accurate description of correlation effects. Some of the present authors showed that, using RPA + SE (SE = single-excitation contributions),

the electronic energy difference between the CP and the LP phase, reduces to about 7 kJ·mol^{-1} [4]. In contrast to the electronic energy, a description of the lattice vibrations at the RPA level of theory is not feasible with the current computational resources. However, an estimate of these vibrations can be obtained at the PBE-D3(BJ) level of theory. Starting from the RPA + SE electronic energy as a function of volume at 0 K [4] and including finite temperature corrections at the PBE-D3(BJ) level of theory, the Helmholtz free energy as a function of volume and at different temperatures can be calculated (see Figure S4). The LP phase is now the most stable phase above 300 K, which is more in line with experimental observations. This underlines that an incorrect prediction of the transition temperature is not necessarily the result of an unreliable description of the lattice dynamics.

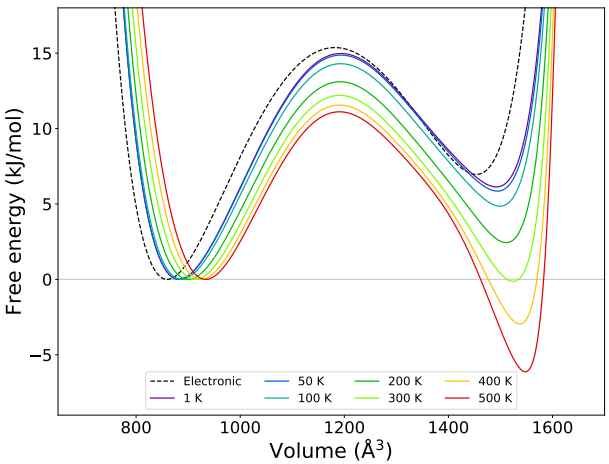

Fig. S4: Helmholtz free energy as a function of the volume at different temperatures (solid lines) and the electronic energy as a function of the volume (black dashed line) using the QHA. The electronic energy is calculated at the RPA + SE level of theory [4], while the finite temperature corrections are obtained at the PBE-D3(BJ) level of theory.

Figure S4 suggests that the PBE-D3(BJ) level of theory is sufficiently accurate to describe the lattice vibrations in MIL-53(Al). Another verification can be obtained by calculating these vibrations explicitly at a higher level of theory. For that purpose, the PBE0-D3(BJ) level of theory is applied, a hybrid functional that adds 25% of Hartree-Fock exchange to the PBE functional [5]. The correspondence between the vibrations at both levels of theory is assessed

by comparing the resulting IR spectra. Although it is theoretically possible to add Hartree-Fock exchange using VASP, the calculation through a plane-wave approach is computationally very demanding. For that purpose, the CRYSTAL17 code was employed, which makes use of atom-centered basis sets [6]. The CRYSTAL calculations were performed starting from the experimental structure determined by Liu et al. [3] at the C2/c space group. After initial geometry optimizations with the space group as the only constraint, the Hessian [7, 8] and IR intensities [9] were calculated. For these calculations, a Gaussian basis set of triple-zeta valence with polarization quality has been used [10] together with a $6 \times 6 \times 6$ Monkhorst-Pack k-mesh. In Figure S5, the resulting IR spectra obtained with the PBE-D3(BJ) and PBE0-D3(BJ) levels of theory are compared with the PBE-D3(BJ) IR spectrum obtained with VASP.

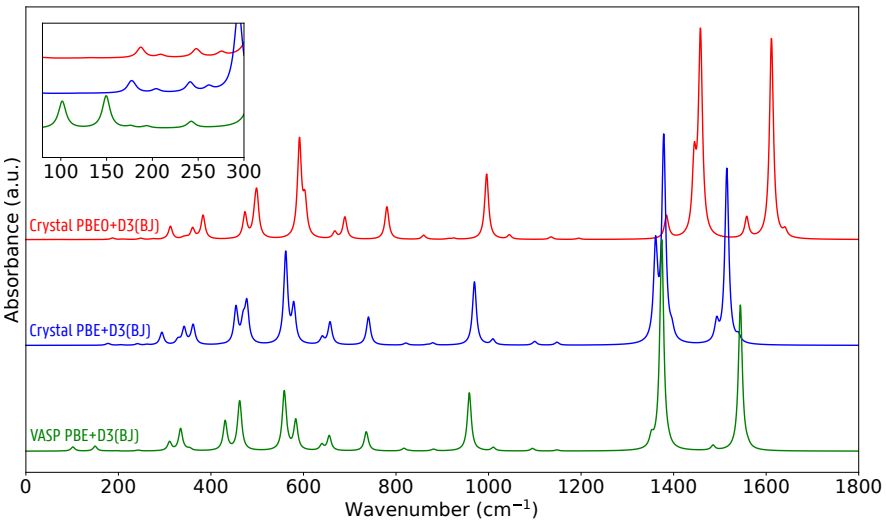

Fig. S5: Theoretical IR spectra of the CP phase of MIL-53(Al) calculated with VASP (green) and CRYSTAL17 (blue) at the PBE-D3(BJ) level of theory and with CRYSTAL17 at the PBE0-D3(BJ) level of theory (red).

A good agreement between the VASP simulation and the CRYSTAL simulation at the PBE-D3(BJ) level of theory is obtained above 300 cm-1, however for lower wavenumbers the spectrum deviates due to symmetry restrictions in the CRYSTAL simulation. Furthermore, the calculated IR spectra at the PBE-D3(BJ) (blue curve) and PBE0-D3(BJ) (red curve) level of theory obtained

with the CRYSTAL17 code are compared. These spectra are in correspondence over the complete frequency range apart from a scaling factor. Based on the calculations in the CRYSTAL17 code, a drastic change in the lattice vibrations is not expected when using a different functional.

S6 Pressure-versus-volume equation of state

An interesting thermodynamic property, which is not treated in the main manuscript, is the pressure-versus-volume ($P(V)$) equation of state [11]. This $P(V)$ equation of state is directly related to the Helmholtz free energy profile by taking its negative derivative with respect to the volume,

$$P(V,T) = -\frac{\partial F(V,T)}{\partial V} \tag{S3}$$

The temperature dependence of the $P(V)$ equation of state is presented in Figure S6. The volume regions in which the material is mechanically stable can readily be obtained by identifying the regions with a negative slope [11]. These regions are delimited by a certain transition pressure, beyond which the material will immediately transition to the other phase. The CP-LP transition pressure at 1 K is given by -204 MPa and its magnitude decreases for increasing temperature towards -184 MPa at 300 K. A negative transition pressure corresponds with pulling the structure, which is not yet feasible experimentally. Nonetheless, our values for the CP-LP transition pressure validate the ones previously obtained by force field molecular dynamics (MD) simulations [12]. The LP-CP transition pressure has a positive value for all temperatures and goes from 32 MPa at 1 K to 61 MPa at 300 K. This is a slight overestimation of the experimentally obtained values of 13–18 MPa at 300 K [13] and force field MD simulations [12]. We have to note that the degree of the fitted polynomial can influence the values of the transition pressures by several MPa.

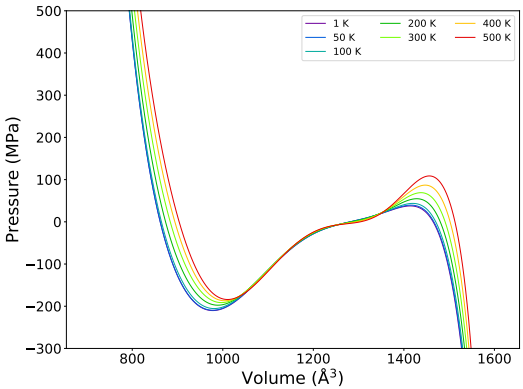

Fig. S6: Pressure-versus-volume equation of state for MIL-53(Al) at different temperatures between 1 K and 500 K as determined from the Helmholtz free energy profile via formula (S3).

S7 Grüneisen parameters

The derivation of volume-frequency relations for the vibrational modes allows to estimate the mode Grüneisen parameters, γ_i. These are defined in the following way:

$$\gamma_i = -\frac{\mathrm{d}\ln\omega_i}{\mathrm{d}\ln V}$$

The mode Grüneisen parameters are thus a measure for the change of vibrational frequencies as a function of the volume. The importance of these Grüneisen parameters arises from their ability to predict whether a material will expand or contract upon temperature changes. A material with mainly negative mode Grüneisen parameters will typically undergo a contraction when the temperature increases (negative thermal expansion (NTE)), while a material with an abundance of positive mode Grüneisen parameters will show positive thermal expansion (PTE) [14]. As MIL-53(Al) has been shown to exhibit PTE [15], we expect a majority of positive mode Grüneisen parameters.

From the definition of mode Grüneisen parameters, it is clear that the first-order derivatives of the vibrational frequencies with respect to the volume are required. For that purpose, we have derived analytical expressions for each vibrational mode by fitting a ninth-order Taylor expansion to each volume-

frequency relation. The choice of the polynomial degree is not trivial, as it can affect the thermodynamic properties considerably (see Section 3.2 in the main manuscript). The resulting mode Grüneisen parameters are presented in Figure S7a, where the parameters assigned to the terahertz vibrations discussed in Section 3.1.2 in the main manuscript are highlighted.

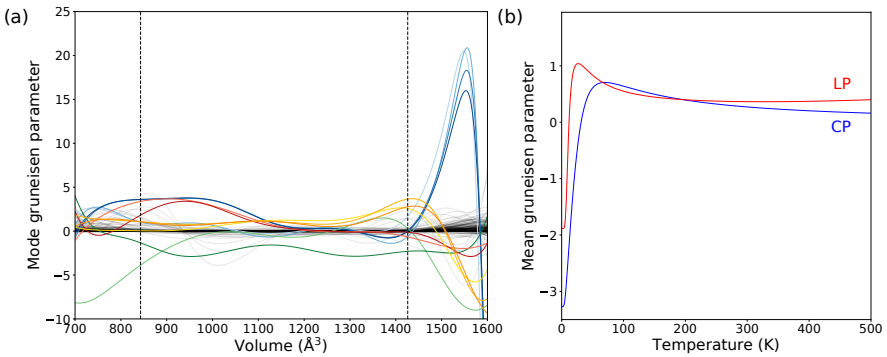

Fig. S7: (a) Mode Grüneisen parameters of the vibrational modes in MIL-53(Al). The terahertz vibrations exposing a large change as a function of the volume are highlighted according to the color scheme in Figure 4 in the main manuscript. Dotted lines indicate the equilibrium volumes of the CP and LP phases obtained from electronic structure calculations. (b) Mean Grüneisen parameters as a function of temperature for the CP (blue) and LP phase (red) structures at their equilibrium volume.

Most vibrational modes have small Grüneisen parameters, except for some low-frequency modes. The mode Grüneisen parameters of the vibrations exhibiting linker rotations (blue curves) show a striking behavior. At very large unit cell volumes, these modes have a very low vibrational frequency, which suddenly drops. This results in a large increase of the mode Grüneisen parameter. At small unit cell volumes, the modes exhibiting linker rotations in the same direction have again a high value for their Grüneisen parameter, as their frequencies drop appreciably for increasing volumes. As these modes have positive values in the volume regions where the CP and LP phases are stable, they contribute greatly to the PTE of MIL-53(Al). This becomes clearer when observing the mean Grüneisen parameters of the CP and the LP phases as a function of the temperature (Figure S7b), which are weighted averages of all mode Grüneisen parameters.

$$\gamma(T) = \sum_{i=1}^{N} \frac{\gamma_i \, C_{V,i}(T)}{C_{V,i}(T)} \tag{S4}$$

Here, $C_{V,n}(T)$ represents the temperature-dependent contribution of mode n to the specific heat capacity at constant volume (see also Section S8). Above 30 K, the mean Grüneisen parameters of both phases have positive values, due to a large positive contribution from the vibrations exhibiting linker rotations, suggesting PTE behavior. Although most vibrational modes have a positive Grüneisen parameter, there are two modes exhibiting large negative values for this parameter over large parts of the considered volume range. It concerns the soft modes discussed in previous paragraph (green curves in Figure S7), which exhibit an increasing vibrational frequency with increasing volume. At small unit cell volumes, these modes have considerably lower vibrational frequencies than the other modes and will thus dominate the vibrational behavior at small volumes. Solely based on the lattice vibrations we can expect NTE for the CP phase at very low temperatures. This can also be concluded from the mean Grüneisen parameters of the CP phase, showing large negative values at low temperatures.

S8 Vibrational contribution to thermodynamic properties

In Section 3.2.2.4 of the main manuscript, the influence of each mode to the thermodynamic properties is presented. The formulas leading to the results reported in the main manuscript are derived here.

S8.1 Specific heat capacity at constant volume

The formula for the specific heat capacity at constant volume can be written as follows:

$$C_V(V,T) = \sum_{i=1}^{N} \frac{(\hbar\omega_i(V))^2}{k_B T^2} \frac{e^{\frac{\hbar\omega_i(V)}{k_B T}}}{\left(e^{\frac{\hbar\omega_i(V)}{k_B T}} - 1\right)^2} \tag{S5}$$

The contribution of each vibrational mode to this specific heat capacity at constant volume corresponds to a specific term in this summation:

$$C_{V,i}(V,T) = \frac{(\hbar\omega_i(V))^2}{k_B T^2} \frac{e^{\frac{\hbar\omega_i(V)}{k_B T}}}{\left(e^{\frac{\hbar\omega_i(V)}{k_B T}} - 1\right)^2} \tag{S6}$$

S8.2 Bulk modulus

The bulk modulus is defined as the second-order derivative of the Helmholtz free energy with respect to the volume multiplied by the volume:

$$K(V,T) = V\frac{\partial^2 F(V,T)}{\partial V^2} \tag{S7}$$

Partitioning of this bulk modulus into vibrational contributions can thus be obtained by determining the second-order derivatives with respect to the volume of the different vibrational contributions to the vibrational free energy. This vibrational free energy contributes to the total free energy and is given by:

$$F(V,T) = E_{el}(V) + F_{vib}(V,T) \tag{S8}$$

$$F_{vib}(V,T) = \sum_{i=1}^{N} \frac{\hbar\omega_i(V)}{2} + k_B T \ln\left(1 - e^{-\frac{\hbar\omega_i(V)}{k_B T}}\right) \tag{S9}$$

By applying formula (S7) to the vibrational free energy in equation (S9), we obtain the following expression:

$$\begin{aligned} V\frac{\partial^2 F_{vib}(V,T)}{\partial V^2} = V \sum_{i=1}^{N} & \frac{-\hbar^2}{k_B T} \frac{e^{-\frac{\hbar\omega_i(V)}{k_B T}}}{\left(1 - e^{-\frac{\hbar\omega_i(V)}{k_B T}}\right)^2} \left(\frac{\mathrm{d}\omega_i(V)}{\mathrm{d}V}\right)^2 \\ & + \hbar\left(\frac{1}{2} + \frac{e^{-\frac{\hbar\omega_i(V)}{k_B T}}}{1 - e^{-\frac{\hbar\omega_i(V)}{k_B T}}}\right) \frac{\mathrm{d}^2\omega_i(V)}{\mathrm{d}V^2} \end{aligned} \tag{S10}$$

In this way, we recognize the different vibrational contributions towards the bulk modulus. It has to be noted the expression of the total Helmholtz free energy also depends on the electronic energy, which will also contribute to the bulk modulus.

S8.3 Volumetric thermal expansion coefficient

Although the formula in the main manuscript to calculate the volumetric thermal expansion coefficient does not depend on separate contributions from the vibrations, it can be approximated through the Grüneisen approach [1]. Within the Grüneisen approach, the volumetric thermal expansion coefficient is calculated by the following formula:

$$\alpha_V(T) = \frac{1}{KV(T)} \sum_{i=1}^{N} \gamma_i C_{V,i}(T) \tag{S11}$$

The volumetric thermal expansion obtained in this way is qualitatively similar to the one presented in Figure 10 in the main manuscript. This Grüneisen approach allows to divide the volumetric expansion coefficient in vibrational contributions:

$$\alpha_{V,i}(T) = \frac{1}{KV(T)} \gamma_i C_{V,i}(T) \tag{S12}$$

References

[1] A. Erba, "On combining temperature and pressure effects on structural properties of crystals with standard ab initio techniques," *J.Chem. Phys.*, vol. 141, no. 12, p. 124115, 2014.

[2] A. E. J. Hoffman, L. Vanduyfhuys, I. Nevjestic, J. Wieme, S. M. J. Rogge, H. Depauw, P. Van Der Voort, H. Vrielinck, and V. Van Speybroeck, "Elucidating the vibrational fingerprint of the flexible metal–organic framework MIL-53(Al) using a combined experimental/computational approach," *J. Phys. Chem. C*, vol. 122, no. 5, pp. 2734–2746, 2018.

[3] Y. Liu, J.-H. Her, A. Dailly, A. J. Ramirez-Cuesta, D. A. Neumann, and C. M. Brown, "Reversible structural transition in MIL-53 with large temperature hysteresis," *J. Am. Chem. Soc.*, vol. 130, no. 35, pp. 11813–11818, 2008.

[4] J. Wieme, K. Lejaeghere, G. Kresse, and V. Van Speybroeck, "Tuning the balance between dispersion and entropy to design temperature-responsive flexible metal-organic frameworks," *Nat. Commun.*, vol. 9, no. 1, p. 4899, 2018.

[5] C. Adamo and V. Barone, "Toward reliable density functional methods without adjustable parameters: The PBE0 model," *J. Chem. Phys.*, vol. 110, no. 13, pp. 6158–6170, 1999.

[6] R. Dovesi, A. Erba, R. Orlando, C. M. Zicovich-Wilson, B. Civalleri, L. Maschio, M. Rérat, S. Casassa, J. Baima, S. Salustro, and B. Kirtman, "Quantum-mechanical condensed matter simulations with crystal," *WIREs: Comput. Mol. Sci.*, vol. 8, p. e1360, 2018.

[7] F. Pascale, C. M. Zicovich-Wilson, F. Lopez Gejo, B. Civalleri, R. Orlando, and R. Dovesi, "The calculation of the vibrational frequencies of crystalline compounds and its implementation in the CRYSTAL code," *J. Comput. Chem.*, vol. 25, no. 6, pp. 888–897, 2004.

[8] C. M. Zicovich-Wilson, F. Pascale, C. Roetti, V. R. Saunders, R. Orlando, and R. Dovesi, "Calculation of the vibration frequencies of α-quartz: The effect of Hamiltonian and basis set," *J. Comput. Chem.*, vol. 25, no. 15, pp. 1873–1881, 2004.

[9] L. Maschio, B. Kirtman, R. Orlando, and M. Rérat, "Ab initio analytical infrared intensities for periodic systems through a coupled perturbed Hartree-Fock/Kohn-Sham method," *J. Chem. Phys.*, vol. 137, no. 20, p. 204113, 2012.

[10] M. F. Peintinger, D. V. Oliveira, and T. Bredow, "Consistent Gaussian basis sets of triple-zeta valence with polarization quality for solid-state calculations," *J. Comput. Chem.*, vol. 34, no. 6, pp. 451–459, 2013.

[11] S. M. J. Rogge, M. Waroquier, and V. Van Speybroeck, "Reliably modeling the mechanical stability of rigid and flexible metal–organic frameworks," *Acc. Chem. Res.*, vol. 51, no. 1, pp. 138–148, 2017.

[12] S. M. J. Rogge, L. Vanduyfhuys, A. Ghysels, M. Waroquier, T. Verstraelen, G. Maurin, and V. Van Speybroeck, "A comparison of barostats for the mechanical characterization of metal–organic frameworks," *J. Chem. Theory Comput.*, vol. 11, no. 12, pp. 5583–5597, 2015.

[13] P. G. Yot, Z. Boudene, J. Macia, D. Granier, L. Vanduyfhuys, T. Verstraelen, V. Van Speybroeck, T. Devic, C. Serre, G. Férey, N. Stock, and G. Maurin, "Metal–organic frameworks as potential shock absorbers: the case of the highly flexible MIL-53(Al)," *Chem. Commun.*, vol. 50, no. 67, pp. 9462–9464, 2014.

[14] G. D. Barrera, J. A. O. Bruno, T. H. K. Barron, and N. L. Allan, "Negative thermal expansion," *J. Phys. Condens. Matter*, vol. 17, no. 4, pp. 217–252, 2005.

[15] C. Nanthamathee, S. Ling, B. Slater, and M. P. Attfield, "Contradistinct thermoresponsive behavior of isostructural MIL-53 type metal–organic frameworks by modifying the framework inorganic anion," *Chem. Mater.*, vol. 27, no. 1, pp. 85–95, 2014.